



Article
scientifique

Revue de la
littérature

2021

Accepted
version

Open
Access

This is an author manuscript post-peer-reviewing (accepted version) of the original publication. The layout of the published version may differ .

Bacillary layer detachment: multimodal imaging and histologic evidence of a novel optical coherence tomography terminology

Ramtohl, Prithvi; Engelbert, Michael; Malcles, Ariane; Gigon, Edward; Miserocchi, Elisabetta; Modorati, Giulio; Cunha de Souza, Eduardo; Besirli, Cagri G; Curcio, Christine A; Freund, K Bailey

How to cite

RAMTOHL, Prithvi et al. Bacillary layer detachment: multimodal imaging and histologic evidence of a novel optical coherence tomography terminology. In: Retina, 2021. doi: 10.1097/IAE.0000000000003217

This publication URL: <https://archive-ouverte.unige.ch/unige:154482>

Publication DOI: [10.1097/IAE.0000000000003217](https://doi.org/10.1097/IAE.0000000000003217)

Financial Disclosures: K.B. Freund is a consultant for Heidelberg Engineering, Zeiss, Genentech, Bayer, Novartis, and Allergan. He receives research support from Genentech/Roche. C. A. Curcio receives research support from Heidelberg Engineering and owns stock of MacRegen. C.G. Besirli is a consultant for iRenix Medical, Janssen, receives equity (iRenix Medical) and royalty (iRenix Medical, ONL Therapeutics), clinical trial support (MeiraGTx, Spark Therapeutics, 4DMT, Regeneron, Novartis), and research support (NIH, The E. Matilda Ziegler Foundation for the Blind, International Retinal Research Foundation). The remaining authors have no financial disclosures.

Corresponding Author: K. Bailey Freund, MD, Vitreous Retina Macula Consultants of New York, 460 Park Avenue, New York, NY 10022; e-mail: kbfnyf@aol.com

Word Count Text: 5216.

Word Count Abstract: 200.

Summary statement: The “bacillary layer detachment” describes a detachment of the photoreceptor inner and outer segments resulting from a split within the inner segment myoids. Utilizing a literature review, we explored associated diagnoses and resolved inconsistent descriptions for the anatomic basis of this finding through correlation with histologic data and retinal imaging.

ABSTRACT

Purpose: To clarify the histologic basis of bacillary layer detachment (BALAD) through a review of current literature and an analysis of retinal imaging.

Methods: We reviewed the literature for previous reports of BALAD. An analysis of retinal images was performed to support anatomic conclusions.

Results: A total of 164 unique patients with BALAD on optical coherence tomography (OCT) were identified from the published literature. Twenty-two underlying etiologies, all associated with subretinal exudation, were identified. Forty-one different OCT terminologies were found. The defining OCT feature of BALAD was a split at the level of the photoreceptor inner segment myoid creating a distinctive intraretinal cavity. Resolution of BALAD was followed by a rapid restoration of the ellipsoid zone. Histology of age-related macular degeneration eyes suggests that individual photoreceptors can shed inner segments. Further, detachment of the entire layer of inner segments is a common postmortem artefact. We propose that BALAD occurs when outwardly directed forces promoting attachment of photoreceptor outer segments to the retinal pigment epithelium exceed the tensile strength of the photoreceptor inner segment myoid.

Conclusion: Our review serves to strengthen the OCT nomenclature “bacillary layer detachment”, based on specific reflectance information obtained by OCT and previously published histologic observations.

Keywords: age-related macular degeneration; anatomy; bacillary layer detachment; histology; macula; multimodal imaging; optical coherence tomography; photoreceptor; retina; retinal detachment; review; subretinal septa; Vogt-Koyanagi-Harada disease.

Introduction

Stratum bacillarum et conorum, the layer of rods and cones, was first described by van

Leeuwenhoek in 1722.¹ Since then, anatomists have used the term “bacillary layer” to

describe the orderly arrangement of photoreceptor inner and outer segments (IS, OS).² Outer segments are made of stacked disks and their tips are surrounded by specialized apical processes of the retinal pigment epithelium (RPE). The photoreceptor IS are divided into two parts: the proximal myoid, near the external limiting membrane (ELM), which comprises ribosomes, smooth endoplasmic reticulum, Golgi complex and rare mitochondria; and the distal ellipsoid zone (near the OS) which has tightly bundled mitochondria.³ In addition to canonical functions of oxidative phosphorylation and calcium buffering, mitochondria were proposed to have optical properties because they are light scatterers.^{4,5}

With advances in ultrahigh-resolution optical coherence tomography (OCT) imaging, new insights into photoreceptor injury can be visualized at a subcellular level. Recently, in a case of macular toxoplasmosis chorioretinitis, Mehta et al. introduced the term “Bacillary Layer Detachment” (BALAD) to describe the separation of the bacillary layer from the remaining retinal layers resulting from an intra-photoreceptor split immediately posterior to the ELM within the photoreceptor IS myoids.⁶ Subsequently, several authors have used this OCT term in various case reports including acute idiopathic maculopathy, blunt ocular trauma, peripapillary pachychoroid syndrome, and Vogt-Koyanagi-Harada (VKH) disease.⁷⁻¹⁰

However, prior descriptions and alternative interpretations of BALAD have created a need for a more generally accepted interpretation regarding the multimodal imaging characteristics of this retinal lesion. In fact, similar OCT findings were described as “photoreceptor

delamination” in neovascular age-related macular degeneration (AMD) and “subretinal septae” in VKH disease.^{11,12} Developing a standardized nomenclature would improve clarity and accuracy of communication and enhance comparability of research results. Furthermore, assessing correctly the retinal fluid location, whether intra- or subretinal, is fundamental as it

is being used in recent neovascular AMD trials as surrogate endpoints and implies different

treatment responses, visual prognosis and pathogenic pathways.¹³⁻¹⁶ Moreover, the prompt recovery of BALAD on multimodal imaging raises questions on mechanisms that drive photoreceptor regeneration, especially the inner segment.

This review aimed to propose an accurate definition of the BALAD through an analysis of multimodal imaging with OCT interpretation supported by recent histologic findings in AMD. We performed a comprehensive review of published cases meeting the current authors' criteria for BALAD, encompassing wide-ranging terminology and descriptors by the original authors. We focused on demographics, clinical and multimodal imaging characteristics, terminologies, and discussed pathophysiologic mechanisms unifying these various chorioretinal disorders. Additionally, we reviewed the current status of rapid bacillary layer recovery as assessed by multimodal imaging techniques and its potential implications for treatments targeting photoreceptor renewal.

Review of the Ophthalmologic Literature

We conducted a systematic search according to Khan et al. 5-step guidelines.¹⁷ In brief, the steps in a systematic review include: (1) framing the questions for a review, (2) identifying the relevant publications, (3) assessing study quality, (4) summarizing the evidence, (5) interpreting the findings. Therefore, we searched PubMed, Medline, Scopus, Science Direct, Cochrane Library, Ovid and Google Scholar from inception through October 2020. We did not restrict the study type or language in the searches. The searched keywords were “bacillary layer detachment”, “atypical subretinal fluid”, “subretinal septae”, “subretinal membranous structures”, “subretinal hyperreflective structures”, “exudative retinal detachment”, “neurosensory detachment”, “cystoid spaces”. Additional relevant articles were found using the “related citations” link in PubMed and through selected article reference lists. After

deduplication, we examined a total of 879 individual articles to confirm whether the given article displayed multimodal retinal images including at least one OCT scan to analyze the retinal morphology. Additional case material derived from the authors' clinics was used to refine specific imaging features. Furthermore, we included intraoperative OCT images showing *in vivo* BALAD development in eyes undergoing subretinal injection of gene therapy during pars plana vitrectomy and reviewed articles displaying similar intraoperative OCT findings. We also reviewed historical textbooks and atlases to trace the origin of the term "bacillary layer".

Demographic Analysis

From 879 articles identified through our systematic search, 123 articles were included, yielding 178 eyes with BALAD identified by OCT in 164 unique patients (see References, and Supplemental References in the Supplemental Digital Content 1, <http://links.lww.com/IAE/B473>). The mean \pm SD patient age was 35.4 ± 14.5 years (range, 10–86 years) and 69 of 138 patients (50%) were female. Three types of OCT were used: spectral-domain OCT (SD-OCT) in 146 eyes (82%), time-domain OCT in 25 eyes (14%) and swept-source OCT (SS-OCT) in 7 eyes (4%). Follow-up OCT images were available in 99 eyes (55.6%) and mean \pm SD follow-up was 167.4 ± 134.3 days (range, 7–1095 days). Mean \pm SD baseline best-corrected visual acuity was 0.98 ± 0.92 LogMAR (Snellen equivalent: 20/191). Underlying etiologies included VKH disease (47%),^{12,18–40,S41–S65} acute posterior multifocal placoid pigment epitheliopathy (APMPPE) (11%),^{S66–S80} sympathetic ophthalmia (7.3%),^{S61,S81–S89} choroidal neovascularization (6.2%),^{11,S90,S91} toxoplasmosis chorioretinitis (5.5%),^{6,10,S92–S97} acute idiopathic maculopathy (5.5%),^{7,S98–S105} immunotherapy-related toxicity (3.7%),^{10,S106–S109} hematological disorders (2.4%),^{S110–S112} posterior scleritis (1.8%),^{10,S47,S113} choroidal metastasis (1.8%),¹⁰ central serous chorioretinopathy (1.8%),^{10,S114}

pan-retinal photocoagulation (0.6%),^{S115} peripapillary pachychoroid syndrome (0.6%),⁹ ocular blunt trauma (0.6%),⁸ uveal effusion syndrome (0.6%),^{S116} choroidal lymphoma (0.6%),^{S117} choroidal osteoma (0.6%),¹⁰ chikungunya-associated uveitis (0.6%),^{S118} laser-induced maculopathy (0.6%),^{S119} bilateral diffuse uveal melanocytic proliferation (0.6%),^{S120} choroidal granuloma (0.6%),^{S121} and preeclampsia (0.6%).^{S122} Choroidal neovascularization included neovascular AMD, idiopathic choroidal neovascularization, and proliferative macular telangiectasia type 2. Immunotherapy-related toxicity included 2 cases associated with ipilimumab (cytotoxic T lymphocyte-associated antigen 4 blocker), one case associated with vemurafenib (BRAF inhibitor) and two cases associated with the combination of dabrafenib (BRAF inhibitor) and trametinib (MEK inhibitor). Hematological disorders included one case of chronic myeloid leukemia, one case of acute myeloid leukemia and one case of thrombotic thrombocytopenic purpura. Central serous chorioretinopathy (CSC) included one case of fibrinous CSC and one case of secondary CSC complicating systemic lupus erythematosus with severe hypertension and renal failure (Table 1).

Terminology in Ophthalmologic Literature

We aimed to identify previous OCT nomenclatures and to review their use in the aforementioned etiologies to better understand the evolution of the terminology. Forty-one different OCT terminologies were found. We summarized them into 7 main categories for greater clarity: (1) subretinal septum/ membrane/ compartment/ loculated space/ cystic space in 61/178 eyes (34.3%), (2) exudative retinal detachment/ subretinal detachment/ swelling of the outer retina/ neurosensory detachment/ elevation of the IS-OS in 49/178 eyes (27.5%), (3) subretinal fluid in 33/178 eyes (18.5%), (4) BALAD in 18/178 eyes (10.1%), (5) subretinal hyperreflective material/ deposit/ proteinaceous exudate in 7/178 eyes (3.9%), (6)

photoreceptor delamination in 7/178 eyes (3.9%), and (7) intraretinal fluid in 3/178 eyes (1.9%).

The first OCT description of BALAD was made by Maruyama and Kishi in a series of 21 patients with VKH disease as “intraretinal fluid accumulation in the outer retina”.^{S123} Yamaguchi *et al.* further confirmed their findings and introduced the term “subretinal septae”, postulating that these septae were comprised of fibrin-like inflammatory products, because they rapidly resolved after steroid therapy.^{S124} Despite the lack of direct histologic correlation for BALAD to date, this hypothesis has gained popularity among retina specialists because eosinophilic exudate containing proteinaceous material has been documented in the subretinal detached area of VKH patients.^{S125–S127} It is only more recently, with the advent of ultrahigh-resolution OCT, that Ishihara *et al.* questioned these findings and proposed the concept of splitting of photoreceptor OS from their IS due to massive fluid accumulation.³⁹

Similar OCT features have been reported in the aforementioned etiologies; however, to our knowledge, no etiologic connection relating similar OCT findings among these diseases has been proposed. In 2018, Mehta *et al.* suggested the term “bacillary layer detachment” in a case of toxoplasmosis chorioretinitis and postulated that the outer retinal split occurred at the level of the IS myoids.⁶ The authors have supported their OCT analysis through correlation with BALAD frequently observed in histological studies of postmortem human eyes (see “Histologic Considerations” below).^{S128}

Optical Coherence Tomography Hallmarks

Bacillary layer detachment has characteristic and predictable features on OCT. Among published cases, BALAD was consistently located at the posterior pole and was foveal in 131/178 eyes (73.6%), parafoveal in 45/178 eyes (25.3%) and peripapillary in 2/178 eyes (1.1%). Colocalization with subretinal and intraretinal fluid was noted in 138/178 eyes (77.5%) and 10/178 eyes (5.6%), respectively. Increased choroidal thickness was documented in 91/97 eyes with reported choroid measurements (93.8%) having a mean \pm SD subfoveal choroidal thickness of $590 \pm 146.7 \mu\text{m}$ (range, 321 – 909 μm).

For the following detailed analysis of outer retinal structures, our review focused on eyes imaged with high-resolution SD-OCT and SS-OCT (n=153 eyes). The OCT hallmarks of the BALAD included: (1) split at the level of the hyporeflective myoid zone creating a distinctive cystic intraretinal space; (2) the “ceiling” or anterior border of BALAD appeared as a hyperreflective granular band, presumably containing remaining fragments of structures corresponding to the myoid zone and regenerating photoreceptor IS and OS; (3) the “floor” or posterior border of the BALAD was delineated by a band of variable reflectivity and thickness appearing as a continuation of the ellipsoid zone of adjacent attached retina. This structure’s composition was presumed to be detached photoreceptor IS and OS remaining adherent to RPE-basal lamina-Bruch membrane (RBB) complex,^{S129} (4) a second hyperreflective band below the BALAD floor was detectable in 47.7% and was continuous with the interdigitation zone of adjacent attached retina; (5) the ELM was distinguishable anterior to the BALAD in 72% of eyes; (6) areas of subretinal fluid under the floor of the BALAD was seen in 50.3%; (7) suspended hyperreflective particles were observed with the BALAD in 77.1% and reflectivity of the BALAD contents was higher compared to that of adjacent subretinal fluid in 90.8%; (8) the BALAD had a distinctive piriform-shaped configuration in 71.9% with acute angles at the base in 77.1% (Figure 1 - 4; see Video 1 in

Supplemental Digital Content 2, <http://links.lww.com/IAE/B474>, which shows three-dimensional OCT-reconstruction of BALAD in acute idiopathic maculopathy; see Figures S1-S4 with corresponding legends in the Supplemental Digital Content 3, <http://links.lww.com/IAE/B475>, which shows additional examples of BALAD on multimodal imaging). In some eyes, focal adhesions between the outer retina and the RBB were identified near the BALAD margin (see Figures S1 - S4 [<http://links.lww.com/IAE/B475>, <http://links.lww.com/IAE/B476>, <http://links.lww.com/IAE/B477>, <http://links.lww.com/IAE/B478>] with corresponding legends in the Supplemental Digital Content 8, <http://links.lww.com/IAE/B480>). These adhesions demonstrated a high degree of outer retinal plasticity present within the central macula. Since detection of these focal lesions often required dense OCT B-scan raster patterns, available only for the authors' case material, their frequency in the published literature was not assessed.

Multimodal Imaging Features

On ophthalmoscopic examination (n=106 eyes), cases were typically described as having subretinal fluid (97.2%) which displayed characteristic round or polygonal yellow borders in 85/106 eyes (80.2%). Lesions that were not detected on ophthalmoscopy (1%), were rarely multifocal (4.7%) and occurred primarily in VKH disease, APMPE, and sympathetic ophthalmia. Lesions consistently faded over time, either spontaneously or following the initiation of anti-inflammatory treatment.

Fundus autofluorescence (FAF) and near-infrared reflectance (NIR) findings were both available in 22/178 eyes (12.4%). Characteristically, the BALAD was hypofluorescent in all cases, either due to masking of RPE FAF by the intra-BALAD exudation or RPE

disruption or both. Near-infrared reflectance demonstrated hyporeflective lesions in all cases.

A thin hyperreflective border surrounded the hyporeflective BALAD in 18/22 eyes (81.8%). Fluorescein angiography (n=92 eyes) was notable for hyperfluorescent pooling of dye (92.4%) within the BALAD cavity which resembled the pattern of serous pigment epithelial detachment (72.4%). Hypofluorescent borders in the late phase corresponded to a yellow margin seen in color fundus photographs, a hyperreflective margin on NIR, and the BALAD angles on OCT. These multimodal imaging findings were not present in adjacent “true” serous retinal detachments. Associated findings on fluorescein angiography included optic disk staining (94.6%), dye pooling beneath adjacent serous retinal detachment (70.7%) and vascular staining (12%). Table 2 summarizes the OCT hallmark features and multimodal imaging findings of BALAD.

Intraoperative Optical Coherence Tomography Features of *in vivo* Bacillary Layer Detachment During Subretinal Gene Therapy Surgery

Intraoperative OCT has demonstrated its utility in patients undergoing subretinal gene therapy to guide viral vector injection and to avoid complications such as sub-RPE or intraretinal injection, foveal overstretching, and macular hole formation.^{S130} With the increased number of subretinal gene therapy cases, additional intraoperative OCT signs were recently described, including the “fleur-de-lis” sign that visualizes early subretinal bleb formation and the “double hyperreflective” sign that detects subretinal air bubbles.^{S131} We reviewed published articles and surgical videos of subretinal gene therapy injection to analyze an unrecognized intraoperative OCT finding that shares overlapping features with BALAD including: (1) an outer retinal split creating a distinctive cystic space (the exact level of separation cannot be firmly located due to lower tissue resolution of intraoperative OCT); (2) the floor of the surgically-induced BALAD was delineated by a faint, thickened, hyperreflective band continuous with the ellipsoid zone of adjacent retina; (3) the floor of the surgically-induced

BALAD could be either adherent or detached from the RPE; (4) the surgically-induced BALAD has a distinctive U-shaped configuration. Illustrations of surgically-induced BALAD are found in Figure 5 (see Video 2, Supplemental Digital Content 9, <http://links.lww.com/IAE/B481>, which shows surgically-induced BALAD during gene therapy surgery).

Origin of the term “Bacillary Layer”

The seventeenth-century Dutch microscopist van Leeuwenhoek was the first to observe the layer of rods and cones when examining a cow’s retina. As early as 1674, in a letter sent to the Royal Society in London, he referred to “*the third tunicle was exceeding thin and tender and having viewed it, I found it also to consist of globules united*”.^{S132} In 1722, he undoubtedly examined photoreceptor outer segments when describing in a frog’s retina “*oblong particles one fourth longer than they were thick*”.^{S133} In 1819, this layer was re-discovered by the Irish pathologist Jacob. At that time, histologic descriptions of the retina have identified two parts including the “medullary layer of the retina” which is attached to the choroid coat and the “vascular layer” next to the vitreous.^{S134} In his “Account of a Membrane in the Eye”, Jacob wrote: “*That it is not the nervous layer which I detach [...] first, because it is impossible to separate that part of the retina [...] and, secondly, because I leave the retina uninjured*”.^{S135} Herein, Jacob provided the first histologic finding of detachment of “*membrana Jacobi*” that was further correlated with the bacillary layer. In 1837, Valentin demonstrated that the Jacob’s membrane consisted of “warts” (“*wärzchen*” in German) which was confirmed by Müller and Henle in 1839 who observed “*rod-shaped bodies*” (“*stabförmigen Körper*” in German).^{S136-S137} In 1840, Hannover identified the second component of the Jacob’s membrane as the “cones” (“*zapfen*” in German).^{S138}

The term “*bacillary layer*” was first introduced by von Brücke in 1847 and derived from the Latin translation (“*stratum bacillosum*”) of the German expression “*schicht der stabförmigen Körper*” (which means “*layer of the rods*”).^{S139} More recently, the term “*bacillary layer*” is found in the Polyak’s treatise “*The Retina*” (1941).² Polyak has described subdivision of the fine structure of the retina and his nomenclature of the retinal layers is widely accepted. In 1995, “*bacillary layer*” appeared on a website based at University of Pennsylvania, an institution contributing seminal retinal neuroscience during that era (http://retina.anatomy.upenn.edu/~rob/lance/retina_gross.html).^{S140,S141} In the modern ophthalmic peer-reviewed literature, Curcio et al. and Spaide and Curcio were the first to use anatomical designations as per Polyak to correlate outer retinal bands on OCT with “*Polyak’s bacillary layer*” on histology.^{3,S142} Bacillary layer is preferred terminology over “*photoreceptor layer*” for just the inner and outer segments, used by many current authors, because photoreceptors are long and highly compartmentalized cells that span several anatomical layers (outer plexiform, Henle fiber and outer nuclear layers). The tissue compartment containing the bacillary layer is the subretinal space, which is a potential space bounded above by the ELM and below by the junctional complexes of the RPE (also called Verhoeff’s membrane).^{S143}

Histologic Considerations

The postmortem occurrence of retinal detachment is a well-known histologic artifact and can manifest either as detachment of the photoreceptor OS from the RPE (a “true” retinal detachment) or as split within the photoreceptor IS myoids (a BALAD) leaving a continuous layer of detached photoreceptor IS fragments and OS remaining adherent to the RPE.^{S144,S145} Histological analysis of AMD eyes has revealed artifactual BALAD,^{S146–S149} as indicated by the authors (Figure 6).^{S146,S148,S149} Collectively, these observations suggest an inherent

weakness in photoreceptor IS structure. In the outer retina, detachments occur at points of structural weakness relative to adjacent layers when separation forces overwhelm physiologic retinal adhesive forces. In the subretinal space, the tight ensheathment of the OS by RPE microvilli may contribute to adhesion by several mechanisms including frictional resistance from the interdigitations, electrostatic interaction between cell membranes, and metabolic supply to ensure the continuous process of OS phagocytosis. Furthermore, the interphotoreceptor matrix, which is a viscous material predominantly composed of glycosaminoglycans, is present in-between photoreceptor OS and strengthens this adhesive process, particularly at the level of photoreceptor matrix sheathes that envelop each photoreceptor OS.^{S150} At the base of the photoreceptor IS, Müller glia are attached to each other and to photoreceptor IS by continuous homotypic and heterotypic *adherens* junctions, respectively, that collectively form the ELM. The ELM serves as a semipermeable diffusion barrier for extracellular components and also a structural support for proper cellular organization, integrity and photoreceptor alignment.^{S151} Therefore, we postulate that inherent weakness in photoreceptor IS structure may manifest as a BALAD *in vivo* during acute subretinal exudation when outwardly directed forces promoting attachment of photoreceptor OS to the RPE exceed the tensile strength of the photoreceptor IS myoids.

Furthermore, it was demonstrated that photoreceptor IS undergo substantial remodeling as degeneration proceeds in AMD. In a systematic review of well-preserved late AMD eyes, Litts et al. found that individual cones can shed IS into the subretinal space.^{S130} Thus, splitting of the IS is not only an histologic artifact but may be part of a spectrum of degenerative changes where BALAD may represent acute and simultaneous shedding of a cluster of IS.^{S149,S152}

Recently, direct clinicopathologic correlation between OCT and histology of outer retinal tubulation in AMD has shown that mitochondria are independent reflectivity sources even when cone IS are severely misaligned and shrunken.^{S153} The reflective border of outer retinal tubulation is attributed to the fission of IS mitochondria, which are normally long and thin, into a myriad of small ovoid organelles that reflect via Mie scattering.⁵ On OCT, the floor of the BALAD is characterized by a faint hyperreflective band continuous with the ellipsoid zone of adjacent retina. Therefore, the optical reflectivity of the BALAD floor may originate from the disordered mitochondria of residual photoreceptor IS ellipsoids remaining adherent to the RBB. Alternative hypotheses of the BALAD floor optical properties may include signal attenuation from the overlying fluid, persistent fragments of the myoids and outer segments adherent to the RBB.

Pathophysiology

The imaging similarities between aforementioned entities suggest overlapping disease processes. We postulate that the main pathophysiological mechanism in BALAD genesis is comparable to exudative retinal detachment and involves breakdown of the RPE component of the outer blood-retina barrier (leaving the ELM component intact). This assumption is consistent with late-phase fluorescein angiograms showing leakage and dye pooling. The outer blood-retina barrier is formed by the tight junctions between neighboring RPE cells and acts to regulate molecular movement of solutes and nutrients from the choroid to the subretinal space.^{S154} Thus, similar pathologic mechanisms occurring in both serous retinal detachment and BALAD may account for the frequency of their colocalization in our review (77.5%). Conversely, the paucity of intraretinal fluid associated with BALAD (5.6%) is likely related to ELM integrity. Other mechanisms of BALAD formation may occur, particularly in

cases of laser-induced BALAD, including RPE insult and pump failure, and thermal injury to the RPE and photoreceptor layer.^{S119,S155}

Our review documented a high proportion of choroidal thickening (93.8%) associated with BALAD. Increased choroidal thickness has been associated with exudative retinal detachments in a wide spectrum of disease processes, including choroidal inflammation, congestion, ischemia, infiltration, neovascularization, and compression. Furthermore, recent studies using OCT angiography have documented choroidal and choriocapillaris flow impairments associated with serous retinal detachment in VKH disease,¹⁹ APMPE,^{S156} sympathetic ophthalmia,^{S157} acute idiopathic maculopathy,^{S158} toxoplasmosis chorioretinitis,^{S159} choroidal tumors,^{S160} and central serous chorioretinopathy.^{S161}

In our review of retinal imaging in BALAD, we qualitatively assessed the optical intensity of the BALAD cavity on OCT as compared to that of adjacent serous retinal detachment and found that the internal reflectivity of BALAD was higher in more than 90%, suggesting different components in these two fluid compartments. Moreover, a high rate of suspended hyperreflective particles was noted within the BALAD cavity and likely represent photoreceptor debris and inflammatory products, including fibrin. In experimental subretinal hemorrhages, it has been demonstrated that fibrin interdigitates with photoreceptor OS.^{S162} We postulate that accumulation of subretinal fibrin may modulate the adhesion between photoreceptor OS and RPE apical microvilli resulting in BALAD in these areas when hydrostatic pressure is exerted by subretinal exudation.

Rapid Bacillary Layer Recovery and Photoreceptor Structure Renewal

Evolution of Bacillary Layer Detachment

Short-term evolution of BALAD was available in 77/178 eyes (43.3%) with a mean duration \pm SD of 10.6 ± 6 days (range, 1–48 days) and was characterized by rapid flattening of the

BALAD on OCT. Long-term follow-up was available in 99/178 eyes (55.6%) and demonstrated progressive restoration of the ellipsoid zone followed by the interdigitation zone. Persistent focal disruptions of the ellipsoid and interdigitation zones were noted in all eyes but were mostly focal attenuation (Figure 3, 4 and S11). Mean final \pm SD best-corrected visual acuity increased to 0.27 ± 0.20 LogMAR (Snellen equivalent: 20/37). The sequential pattern of evolution of the floor of BALAD (presumably containing split photoreceptor myoids, ellipsoids and outer segments) provided direct morphological evidence that injured photoreceptors may show some degree of spontaneous inner and outer segment regeneration. A similar sequence of transient bacillary layer disruption followed by rapid restoration has been demonstrated using adaptive optics imaging in several retinal entities including multiple evanescent white dot syndrome,^{S163} acute idiopathic blind spot enlargement,^{S164} acute macular neuroretinopathy,^{S165} central serous chorioretinopathy,^{S166} or after retinal detachment surgery.^{S167} However, these studies have mainly focused their high-resolution imaging analysis on the photoreceptor OS mosaic, showing progressive increased density and realignment along with visual function improvement. In BALAD, the rapid functional improvement and structural recovery of the bacillary layer on multimodal imaging would imply additional mechanisms of photoreceptor IS renewal, including regenerating mitochondria, Golgi apparatus, and endoplasmic reticulum. Shedding IS and loss of myoids are part of a one-way cone degenerative process occurring in AMD eyes.^{S128} Considering that BALAD designates an intra-photoreceptor fracture at the level of the myoid, IS recovery may provide additional insights into photoreceptor regenerative pathways.

Dynamics of Inner Segment Organelle Recovery After Photoreceptor Injury

Photoreceptor mitochondria are mostly confined to the distal ellipsoid portion of the photoreceptor IS,⁴ and their oxygenation is highly dependent from the choroidal

circulation.^{S168} Mitochondria are semi-autonomous organelles that contain their own genome and protein translation machinery. Their dominant role is to ensure photoreceptor metabolic requirements by producing adenosine triphosphate (ATP) through oxidative phosphorylation. They are also mobile organelles that constantly undergo cyclic morphological changes including fusion and fission through highly regulated processes to respond to metabolic needs or environmental stress.^{S169,S170} Fusion allows healthy and mildly damaged mitochondria to fuse to generate interconnected organelles, while fission produces depolarized fragments from severely impaired mitochondria that are further eliminated by a programmed autophagy termed mitophagy.^{S170} These dynamic processes contributing to cell health and mitochondrial dysfunction has been associated with retinal dystrophies.^{S171} Recent investigations in animal models have demonstrated daily cone mitochondrial structural and functional changes to supply higher energy demands in darkness.^{S172,S173} Adaptative mechanisms include mitochondrial biogenesis preceding the increased cone metabolic activity and the number of mitochondria in single cones. Moreover, it has been suggested that normal cones can selectively export damaged mitochondria away from the ellipsoid region and that this selective mitochondrial movement is enhanced by mitochondrial stress.^{S174} Collectively, these data highlight intrinsic autoregulatory mechanisms of IS mitochondria and the remarkable regenerative potential of photoreceptor organelles.

Electron microscopy studies of IS mitochondria after experimental retinal detachment provided evidence of rapid regeneration following reattachment.^{S175,S176} This finding has been confirmed using immunocytochemical labeling of the cytochrome oxidase, which is a key enzyme involved in ATP synthesis within IS mitochondria.^{S177} These regenerative changes were negatively correlated with the duration and height of the detachment. Greater height indicates greater distance of the IS from the choroid, thereby reducing oxygen and nutrient delivery.^{S177-S179} In our analysis, BALAD was remarkable for its short-term duration and the

persistent proximity between the IS ellipsoids and the RPE, which may contribute to the relative preservation of the IS mitochondria oxygenation from the choroid during the acute phase and further promote the rapid recovery during the follow-up by allowing uninterrupted delivery of glucose and other metabolic intermediates. Alternative recovery strategies during the first days of retinal detachment included the decompartmentalization of the rough endoplasmic reticulum and Golgi apparatus in the myoid.^{S175,S176} Thus photoreceptor survival may be enhanced by a decrease in the metabolic cost of maintaining the highly compartmentalized and polarized IS organelles. Moreover, retinal reattachment allowed the re-growth of photoreceptor axons through selective expression of molecules implicated in targeted synaptogenesis.^{S180}

Photoreceptor Metabolism and Inner and Outer Segment Regeneration after Bacillary Layer Detachment

Unlike most other terminally differentiated neurons, photoreceptors have massive biosynthetic requirements that rival rapidly dividing cells. Baseline physiologic requirements place an exceedingly high metabolic demand on photoreceptors to generate the energy and macromolecules necessary for normal visual function and survival.^{S181} Daily shedding of spent disks requires rapid replacement of ~10 % of OS in rods and cones, requiring anabolic production of lipids, proteins, and nucleic acids.^{S182} To meet this high biosynthetic requirement for OS recycling, photoreceptors have developed unique metabolic adaptations, including aerobic glycolysis, or the conversion of glucose to lactate despite the presence of oxygen.^{S183,S184} Studies have demonstrated that 80–90% of the glucose delivered to the outer retina is converted to lactate via aerobic glycolysis.^{S181} Aerobic glycolysis, or the Warburg effect, is a hallmark of rapidly dividing cells, including tumor cells supporting unrestrained proliferation.^{S185} By preferentially utilizing aerobic glycolysis, photoreceptors can rapidly

generate metabolic intermediates that are preferentially shuttled to lipid, amino acid, and nucleic acid production pathways.^{S184} The critical role of the Warburg effect in photoreceptor metabolism was recently demonstrated by Chinchore et al. who showed that reducing the expression of key aerobic glycolysis enzymes diminish the ability to maintain OS.^{S183} The unique ability to perform aerobic glycolysis underscores that photoreceptors are metabolically wired to replenish and regenerate cellular components including organelles and membranes required for the assembly of IS and OS.^{S181-S185} In ground squirrels, hibernation leads to cone OS shortening, decreased mitochondrial size and numbers, depletion of ribosomes, and fragmentation of Golgi complex, all of which recover when hibernation is terminated, with rapid regeneration of mitochondria, ribosomes, Golgi complex in IS followed by the OS regeneration.^{S186} Similarly, ample clinical evidence supports that photoreceptor IS and OS may exhibit spontaneous recovery after injury. Longitudinal OCT assessment of photoreceptors after retinal detachment surgery has demonstrated progressive restoration of the ellipsoid zone of IS followed by OS interdigitation with apical processes of the RPE.^{S167} A similar sequential pattern of photoreceptor IS and OS healing has been reported after macular hole surgery.^{S187}

Strengths and Limitations

Strengths of our literature review include multimodal imaging confluence of a large number of patients with different etiologies, thorough correlation of OCT-derived anatomical information with previously published histologic observations of the retina, and validation of a novel descriptive terminology based on specific reflectance information obtained by OCT combined with the widely accepted nomenclature of retinal layers as per Polyak. We have also incorporated new concepts from experimental studies of retinal metabolism and injury response. Furthermore, we proposed a novel acronym “BALAD” (BAcillary LAYer

Detachment) to avoid confusion with basal laminar deposits (BLamD) and basal linear deposits (BLinD) in AMD, which are both called “BLD” in older literature.^{S188,S189}

Limitations include the lack of direct histologic analysis of BALAD. However, such a correlation is particularly challenging, considering the transient nature of BALAD, the relatively young age of affected population and the histologic artifacts that impair retinal examinations. The histologic reports used to validate this nomenclature mostly showed postmortem artifactual BALAD in AMD patients, with one report providing evidence that individual IS shed even in intact retinas.^{S128} Therefore, extrapolation from pathology to OCT should be cautious. However, these reports demonstrated an inherent weakness in photoreceptor IS and further support our OCT analysis.

Conclusions and Perspectives

Within two decades, the terminology evolved from a more speculative OCT feature as “proteinaceous exudate” to a pure descriptive disease manifestation as “bacillary layer detachment”. In contrast to previous appellations such as “subretinal septa”, “subretinal membrane” or “subretinal compartment”, the term BALAD emphasizes on the importance of outer retinal morphological changes on OCT. It provides new insights into the retinal layers that are affected and implies distinctive pathophysiological pathways in disease processes. It also highlights that when normal outer retinal structure is restored, this process may include the regeneration of IS myoid and IS ellipsoid. The term “bacillary layer” allows for future specification concerning the exact level of photoreceptor IS splitting as OCT technology continues to evolve. Moreover, the term “detachment” has been preferred over “schisis”, because it coincides with the original observation from Jacob.^{S135} Furthermore, no connecting fibers or strands are found in BALAD as opposed to retinoschisis on OCT.^{S190} Illustrations of concurrent BALAD with Henle fiber layer schisis and edema are found in Figure 7 (see

Figures S5 with corresponding legend in the Supplemental Digital Content 3 which shows additional examples of BALAD with adjacent Henle fiber layer schisis).

Acute VKH disease and acute CSC are two common disorders affecting the choroid and the RPE. These two conditions share similar multimodal imaging features, including serous retinal detachments and increased choroidal thickness on OCT, dye leakage on fluorescein angiography and early hypofluorescence of the choriocapillaris on indocyanine green angiography.^{S191} However, their pathogenic mechanisms are distinct; while acute VKH disease is characterized by non-necrotizing granulomatous inflammation of the uveal tract, acute CSC is likely related to choroidal venous insufficiency with choroidal vascular hyperpermeability.^{22,S192} Based on our literature review and given the paucity of BALAD reported in acute CSC, we proposed that the occurrence of BALAD on OCT may help distinguishing acute VKH disease from acute CSC, especially in cases of atypical, bilateral CSC with bullous exudative retinal detachments.^{S193}

Our review also expanded the intraoperative OCT findings in patients undergoing subretinal gene therapy surgery. We provided an in-depth OCT analysis of surgically-induced BALAD published in the literature and supported our observation by well-illustrated personal cases. Recognition of this distinctive intraoperative OCT feature may help surgeons to monitor subretinal injection and improve gene therapy delivery protocols. The mechanism of surgically-induced BALAD is likely comparable to aforementioned pathophysiologic processes. The injection of subretinal fluid through a retinotomy is similar to exudative fluid originating from the choroid. Additional mechanisms may be suggested, including the degree of outer retinal atrophy in the area of injection that modulates normal retinal adhesion and shallow penetration of the needle tip that can result in intraretinal hydration.

The aim of this review was to propose a nomenclature that is internally consistent and based on anatomical ground truth. The need for a logical approach to the OCT terminology is

required to standardize future researches. In the case of BALAD, new terminology connected this clinical feature to a large literature of mechanistic studies.

References

1. **Historical review. *Acta Ophthalmologica*. 1935;13(S6):13-28. doi:10.1111/J.1755-3768.1935.Tb04724.X**
2. **Polyak SL. The retina; the anatomy and the histology of the retina in man, ape, and monkey, including the consideration of visual functions, the history of physiological optics, and the histological laboratory technique. Univ. Of Chicago Press; 1941.**
3. **Spaide RF, Curcio CA. Anatomical correlates to the bands seen in the outer retina by optical coherence tomography: literature review and model. *Retina*. 2011;31(8):1609-1619. doi:10.1097/IAE.0b013e3182247535**
4. **Hoang QV, Linsenmeier RA, Chung CK, Curcio CA. Photoreceptor inner segments in monkey and human retina: mitochondrial density, optics, and regional variation. *Vis Neurosci*. 2002;19(4):395-407. doi:10.1017/S0952523802194028**
5. **Litts KM, Zhang Y, Freund KB, Curcio CA. Optical coherence tomography and histology of age-related macular degeneration support mitochondria as reflectivity sources. *Retina*. 2018;38(3):445-461. doi:10.1097/IAE.0000000000001946**
6. **Mehta N, Chong J, Tsui E, et al. Presumed foveal bacillary layer detachment in a patient with toxoplasmosis chorioretinitis and pachychoroid disease. *Retinal Cases***

& Brief Reports. Published Online August 2018:1.

doi:10.1097/ICB.0000000000000817

7. Fernández-Avellaneda P, Breazzano MP, Fragiotta S, et al. Bacillary layer detachment overlying reduced choriocapillaris flow in acute idiopathic maculopathy. *Retinal Cases & Brief Reports*. Published Online November 2019:1. doi:10.1097/ICB.0000000000000943
8. Tekin K, Teke MY. Bacillary layer detachment: a novel optical coherence tomography finding as part of blunt eye trauma. *Clin Exp Optom*. 2019;102(3):343-344. doi:10.1111/Cxo.12876
9. Ramtohul P, Comet A, Denis D. Bacillary layer detachment in peripapillary pachychoroid syndrome. *Oph Retina*. 2020;4(6):587. doi:10.1016/J.Oret.2020.01.017
10. Cicinelli MV, Giuffré C, Marchese A, et al. The bacillary detachment in posterior segment ocular diseases. *Ophthalmology Retina*. 2020;4(4):454-456. doi:10.1016/J.Oret.2019.12.003
11. Liakopoulos S, Keane PA, Ristau T, et al. Atypical outer retinal fluid accumulation in choroidal neovascularization: a novel OCT finding. *Ophthalmic Surg Lasers Imaging Retina*. 2013;44(6 (Suppl)):S11-S18. doi:10.3928/23258160-20131101-03
12. Lin D, Chen W, Zhang G, et al. Comparison of the optical coherence tomographic characters between acute Vogt-Koyanagi-Harada disease and acute central serous chorioretinopathy. *BMC Ophthalmol*. 2014;14(1):87. doi:10.1186/1471-2415-14-87

13. Simader C, Ritter M, Bolz M, et al. Morphologic parameters relevant for visual outcome during anti-angiogenic therapy of neovascular age-related macular degeneration. *Ophthalmology*. 2014;121(6):1237-1245.
doi:10.1016/J.Ophtha.2013.12.029
14. Gianniou C, Dirani A, Jang L, Mantel I. Refractory intraretinal or subretinal fluid in neovascular age-related macular degeneration treated with intravitreal ranibizumab: functional and structural outcome. *Retina*. 2015;35(6):1195-1201.
doi:10.1097/IAE.0000000000000465
15. Spaide RF. Retinal vascular cystoid macular edema: review and new theory. *Retina*. 2016;36(10):1823-1842. doi:10.1097/IAE.0000000000001158
16. Dugel PU, Koh A, Ogura Y, et al. HAWK and HARRIER: phase 3, multicenter, randomized, double-masked trials of brolucizumab for neovascular age-related macular degeneration. *Ophthalmology*. 2020;127(1):72-84.
doi:10.1016/J.Ophtha.2019.04.017
17. Khan KS, Kunz R, Kleijnen J, Antes G. Five steps to conducting a systematic review. *J R Soc Med*. 2003;96(3):118-121.
18. Agarwal A, Freund KB, Kumar A, et al. Bacillary layer detachment in acute Vogt–Koyanagi–Harada disease: a novel swept-source optical coherence tomography analysis. *Retina*. 2020;Publish Ahead Of Print.
doi:10.1097/IAE.0000000000002914
19. Aggarwal K, Agarwal A, Mahajan S, et al. The role of optical coherence tomography angiography in the diagnosis and management of acute Vogt–

- Koyanagi–Harada disease. *Ocular Immunology and Inflammation*. 2018;26(1):142-153. doi:10.1080/09273948.2016.1195001
20. Anderson EW, El Khoury L, Schwartzman-Morris JS, et al. Tuberculous choroiditis in patient with Vogt–Koyanagi–Harada disease. *Retinal Cases & Brief Reports*. 2018;Publish Ahead Of Print. doi:10.1097/ICB.0000000000000791
21. Arevalo JF, Lasave AF, Gupta V, et al. Clinical outcomes of patients with Vogt–Koyanagi–Harada disease over 12 years at a tertiary center. *Ocular Immunology and Inflammation*. 2016;24(5):521-529. doi:10.3109/09273948.2015.1025984
22. Attia S, Khochtali S, Kahloun R, et al. Vogt–Koyanagi–Harada disease. *Expert Review of Ophthalmology*. 2012;7(6):565-585. doi:10.1586/Eop.12.63
23. Bae SS, Forooghian F. Optical coherence tomography-based quantification of photoreceptor injury and recovery in Vogt–Koyanagi–Harada uveitis. *Ocular Immunology and Inflammation*. 2017;25(3):338-343. doi:10.3109/09273948.2015.1125510
24. Bhende M, Shetty S, Parthasarathy M, Ramya S. Optical coherence tomography: a guide to interpretation of common macular diseases. *Indian J Ophthalmol*. 2018;66(1):20. doi:10.4103/Ijo.IJO_902_17
25. Chee S-P, Chan S-WN, Jap A. Comparison of enhanced depth imaging and swept source optical coherence tomography in assessment of choroidal thickness in Vogt–Koyanagi–Harada disease. *Ocular Immunology and Inflammation*. 2017;25(4):528-532. doi:10.3109/09273948.2016.1151896

26. Dogan B, Erol MK, Cengiz A. Vogt–Koyanagi–Harada disease following BCG vaccination and tuberculosis. *Springerplus*. 2016;5(1):603. doi:10.1186/S40064-016-2223-4
27. Egawa M, Mitamura Y, Akaiwa K, et al. Changes of choroidal structure after corticosteroid treatment in eyes with Vogt–Koyanagi–Harada disease. *Br J Ophthalmol*. 2016;100(12):1646-1650. doi:10.1136/Bjophthalmol-2015-307734
28. Errera M-H, Levinson RD, Fardeau C, et al. Late posterior segment relapses in a series of Vogt-Koyanagi-Harada disease. *Acta Ophthalmol*. 2015;93(6):E509-E510. doi:10.1111/Aos.12640
29. For The OCTA Study Group, Aggarwal K, Agarwal A, et al. Distinguishing features of acute Vogt-Koyanagi-Harada disease and acute central serous chorioretinopathy on optical coherence tomography angiography and en face optical coherence tomography imaging. *J Ophthalm Inflamm Infect*. 2017;7(1):3. doi:10.1186/S12348-016-0122-Z
30. Gill I, Ziouzina O, Kalisiak M, Fielden M. Probable Vogt-Koyanagi-Harada disease with granulomatous tattoo-related dermatitis. *Canadian Journal Of Ophthalmology*. 2018;53(5):E179-E182. doi:10.1016/J.Jcjo.2018.01.012
31. Hashizume K, Imamura Y, Fujiwara T, et al. Retinal pigment epithelium undulations in acute stage of Vogt-Koyanagi-Harada disease: biomarker for functional outcomes after high-dose steroid therapy. *Retina*. 2016;36(2):415-421. doi:10.1097/IAE.0000000000000728
32. Hirooka K, Saito W, Namba K, et al. Relationship between choroidal blood flow velocity and choroidal thickness during systemic corticosteroid therapy for Vogt–

- Koyanagi–Harada disease. *Graefes Arch Clin Exp Ophthalmol*. 2015;253(4):609-617. doi:10.1007/S00417-014-2927-5
33. Hosoda Y, Hayashi H, Kuriyama S. Posterior subtenon triamcinolone acetonide injection as a primary treatment in eyes with acute Vogt–Koyanagi–Harada disease. *Br J Ophthalmol*. 2015;99(9):1211-1214. doi:10.1136/Bjophthalmol-2014-306244
34. Hosoda Y, Uji A, Hangai M, et al. Relationship between retinal lesions and inward choroidal bulging in Vogt-Koyanagi-Harada disease. *American Journal of Ophthalmology*. 2014;157(5):1056-1063.E1. doi:10.1016/J.Ajo.2014.01.015
35. Hsu Y-R, Huang JC-C, Tao Y, et al. Noninfectious uveitis in the Asia–Pacific region. *Eye*. 2019;33(1):66-77. doi:10.1038/S41433-018-0223-Z
36. Huang G, Peng J, Ye Z, et al. Multispectral image analysis in Vogt-Koyanagi-Harada disease. *Acta Ophthalmol*. 2018;96(4):411-419. doi:10.1111/Aos.13606
37. Ingolotti M, Schlaen BA, Roig Melo-Granados EA, et al. Azathioprine during the first trimester of pregnancy in a patient with Vogt-Koyanagi-Harada disease: a multimodal imaging follow-up study. *Am J Case Rep*. 2019;20:300-305. doi:10.12659/AJCR.914281
38. Invernizzi A, Cozzi M, Staurenghi G. Optical coherence tomography and optical coherence tomography angiography in uveitis: a review. *Clin Experiment Ophthalmol*. 2019;47(3):357-371. doi:10.1111/Ceo.13470

39. Ishihara K, Hangai M, Kita M, Yoshimura N. Acute Vogt–Koyanagi–Harada disease in enhanced spectral-domain optical coherence tomography. *Ophthalmology*. 2009;116(9):1799-1807. doi:10.1016/J.Ophtha.2009.04.002
40. Kawano H, Sonoda S, Yamashita T, et al. Relative changes in luminal and stromal areas of choroid determined by binarization of edi-oct images in eyes with Vogt-Koyanagi-Harada disease after treatment. *Graefes Arch Clin Exp Ophthalmol*. 2016;254(3):421-426. doi:10.1007/S00417-016-3283-4

Figure Legends

Figure 1. Adapted from Fernández-Avellaneda P et al.⁷ Bacillary layer detachment associated with acute idiopathic maculopathy and proposed annotation system.

- A.** Color fundus photograph of a 31-year-old man with vision loss in his right eye shows a yellowish foveal elevation with a thin, peripheral, yellow border (*white arrowhead*).
- B.** Spectral domain optical coherence tomography (SD-OCT) B-scan shows a foveal bacillary layer detachment (BALAD) with small areas of surrounding serous retinal detachment. Note the hyporeflective loss of normal inner choroidal architecture beneath the areas of overlying retinal changes. The white dashed box indicates the area shown in the magnified view (C).
- C.** Magnified SD-OCT B-scan of BALAD. The outer retinal split occurs at the level of the hyporeflective myoid zone (*MZ, green arrowhead*) beneath the external limiting membrane (*ELM, blue arrowhead*) leaving the remaining photoreceptor

layers (fragments of the MZ, ellipsoid zone (*EZ*, *red arrowhead*) and interdigitation zone (*IZ*, *orange arrowhead*)) adherent to the retinal pigment epithelium-basal lamina-Bruch membrane complex (*RBB*, *yellow arrowhead*) at the base of the BALAD. The “ceiling” or anterior border of the BALAD (*white arrowhead*) appears as a hyperreflective granular band, presumably containing remaining fragments of the myoid zone and regenerating photoreceptor inner and outer segments. The “floor” or posterior border of the BALAD (*white arrowhead*) is delimited by a thickened band of heterogenous reflectivity. The anterior portion of BALAD floor is continuous with the ellipsoid zone (*EZ*, *red arrowhead*) in adjacent attached retina. Note the hyperreflective material within the cystoid space created by the BALAD. The annotations using colored labels for specific retinal structures is continued throughout the remaining figures.

Figure 2. Bacillary layer detachment associated with exudative neovascular age-related macular degeneration.

- A. Confocal color fundus photograph of a 61-year-old woman with recent vision loss in her right eye shows greyish pigment epithelial detachment with subretinal fluid.
- B. Spectral domain optical coherence tomography (SD-OCT) B-scan shows a pigment epithelial detachment (PED) with subretinal hyperreflective material and subretinal fluid consistent with exudative type 1 macular neovascularization. No bacillary layer detachment (BALAD) is apparent at presentation. The inset image is the corresponding near-infrared reflectance (NIR) image with the green line indicating the location of the SD-OCT B-scan.
- C. *En face* swept-source optical coherence tomography angiography projection (top) using the retinal pigment epithelium and Bruch’s membrane as segmentation boundaries

shown as yellow dashed lines in the corresponding OCT B-scan with red flow signal overlay (bottom) confirms type 1 macular neovascularization.

D. Six weeks after intravitreal injection of aflibercept (2.0mg/0.05ml), follow-up confocal color fundus photograph shows a larger PED.

E and F. Follow-up tracked SD-OCT B-scan acquired on a prototype high-resolution device (HR-OCT, Spectralis, Heidelberg Engineering, Heidelberg, Germany) (**E**) and magnified view (**F**) show a foveal BALAD. The outer retinal split occurs at the level of the hyporeflective myoid zone (*MZ, green arrowhead*) beneath the external limiting membrane (*ELM, blue arrowhead*) leaving the remaining photoreceptor layers (ellipsoid zone (*EZ, red arrowhead*) and interdigitation zone (*IZ, orange arrowhead*)) adherent to subretinal hyperreflective material anterior to the retinal pigment epithelium-basal lamina-Bruch membrane complex (*RBB, yellow arrowhead*) at the base of the BALAD. The “ceiling” or anterior border of the BALAD (*white arrowhead*) appears as a hyperreflective granular band, presumably containing remaining fragments of the myoid zone and regenerating photoreceptor inner and outer segments. The anterior portion of BALAD floor (*white arrowhead*) is continuous with the ellipsoid zone (*EZ, red arrowhead*) within adjacent attached retina. The inset NIR image with the green line indicates the location of the HR-OCT B-scan.

Figure 3. Meticulous analysis of the bacillary layer detachment border in Vogt-Koyanagi-Harada disease using a dense (11 μ m interscan distance) optical coherence tomography raster pattern.

A. Spectral domain optical coherence tomography (SD-OCT) of nascent bacillary layer detachment (BALAD) shows hyperreflective material accumulation (*white arrowhead*) at the level of the hyporeflective myoid zone (*MZ, green arrowhead*) with

inward bowing of the external limiting membrane (*ELM, blue arrowhead*) and focal attenuation of the underlying ellipsoid zone (*EZ, red arrowhead*). The floor of the nascent BALAD (*f-BALAD, white arrowhead*) is adherent to the retinal pigment epithelium-basal lamina-Bruch membrane complex (*RBB, yellow arrowhead*). Note the distinctive hyperreflective border (*black arrowhead*) of the BALAD on near-infrared reflectance (NIR). The green arrow in the NIR image (right) indicates the location of the spectral domain optical coherence tomography (SD-OCT) B-scan (left).

B. Adjacent inferior SD-OCT B-scan demonstrates further enlargement of the hyporeflective myoid zone splitting creating the BALAD (*white arrowhead*). There is increased reflectivity of the outer nuclear layer and portions of the Henle fiber layer overlying the BALAD.

C and D. Adjacent inferior SD-OCT B-scans show gradual enlargement of the BALAD. The ceiling of the BALAD (*c-BALAD, white arrowhead*) is apparent as a granular hyperreflective band. The floor of the BALAD (*f-BALAD, white arrowhead*) is continuous with the ellipsoid zone of adjacent retina. There is a linear, hyperreflective structure (*white dashed arrow in D*) overlying the floor of the BALAD that appears to represent fragments of photoreceptor inner segment myoids.

E. One month later, following treatment with oral corticosteroids, tracked SD-OCT B-scan corresponding to (**D**) shows resolution of the BALAD. The ELM is intact. There are focal attenuations of the EZ and IZ.

Figure 4. Serial spectral domain optical coherence tomography of bacillary layer detachment resolution in Vogt-Koyanagi-Harada disease.

A. Baseline near-infrared reflectance (NIR, left) and spectral domain optical coherence tomography (SD-OCT) B-scans of a 46-year-old female with a 3-day history of decreased visual acuity in her right eye. There is a dome-shaped foveal bacillary layer detachment (BALAD). The ceiling of the BALAD appears as a faint hyperreflective band (*white arrowhead*). The floor of the BALAD is characterized by a faint, irregular, hyperreflective band (*white arrowhead*) continuous with the ellipsoid zone (*EZ, red arrowhead*) in adjacent retina and adherent to the retinal pigment epithelium-basal lamina-Bruch membrane complex (*RBB, yellow arrowhead*). The green line indicates the location of the SD-OCT B-scan. Note the distinctive hyperreflective border of the BALAD on NIR (*black arrowhead*).

B. Two days after the start of steroid therapy, the external limiting membrane (*ELM, blue arrowhead*) is clearly traceable over the BALAD. The anterior border of the BALAD is delineated by a sharp hyperreflective line (*white arrowhead*) presumably containing regenerating photoreceptor inner segments (*IS*) and outer segments (*OS*). Fragments of *IS* and *OS* (*red arrowheads*) are visible anterior to the retinal pigment epithelium-basal lamina-Bruch membrane complex (*RBB, yellow arrowhead*).

C and D. Five days (**C**) and seven days (**D**) after the start of steroid therapy, the external limiting membrane (*ELM, blue arrowhead*) is still intact over the BALAD. Resolving fragments of degenerating *IS* and *OS* constitute a granular, discontinuous, hyperreflective band (*red arrowheads*) anterior to the *RBB* (*yellow arrowhead*).

E and F. Ten days (**E**) and 90 days (**F**) after the start of steroid therapy, there is a gradual reconstitution of the ellipsoid zone (*EZ, red arrowhead*) with persistent focal disruptions.

Figure 5. Surgically-induced bacillary layer detachment during subretinal gene therapy injection.

- A.** Preoperative near-infrared reflectance (NIR, left) and spectral domain optical coherence tomography (SD-OCT, right) of a 12-year-old girl with biallelic RPE65-mediated inherited retinal disease. Note the preservation of the foveal external limiting membrane and ellipsoid zone. The green line indicates the location of the SD-OCT B-scan.
- B.** Color fundus photograph (left) and intraoperative SD-OCT (right) obtained during subretinal gene therapy with voretigene neparvovec-rzyl. The horizontal SD-OCT scan demonstrates areas of subretinal fluid (*asterisks*) and bacillary layer detachment (BALAD, *white arrowhead*). There are multiple areas of Henle fiber layer (HFL) schisis and edema (*white dashed arrow*). The white dashed box is a magnified view of the BALAD. The ceiling of the BALAD (*white arrowhead*) appears as a thickened hyperreflective band between areas of adjacent HFL schisis and edema. The floor of the BALAD (*white arrowhead*) is adherent to the retinal pigment epithelium-basal lamina-Bruch membrane complex (*RBB*, *yellow arrowhead*) and continuous with the ellipsoid zone (*EZ*, *red arrowhead*) in adjacent retina.
- C.** Color fundus photography and intraoperative SD-OCT obtained during subretinal gene therapy with voretigene neparvovec-rzyl. Adjacent horizontal SD-OCT B-scan shows 2 U-shaped BALADs (*white arrowheads*). The white dashed box is a magnified view of the BALAD. The “floating” detached bacillary layer (*white arrowheads*) show no adhesion to the retinal pigment epithelium-basal lamina-Bruch membrane complex (*RBB*, *yellow arrowhead*).

Figure 6. Modified from Chen L. et al.^{S194} Artfactual bacillary layer detachment in post-mortem histology.

A. Optical coherence tomography B-scan acquired 1 year before patient death showing an extensive subfoveal shallow irregular retinal pigment epithelium (RPE) elevation harboring type 1 macular neovascularization (*yellow arrowheads*), secondary to age-related macular degeneration. Retina is physically intact.

B-D. Post-mortem histology. Asterisks, bacillary layer detachment (BALAD) at the level of inner segment myoids, with outer segments remaining attached to the RPE. Green arrowheads in (**C**) and (**D**), external limiting membrane. Tissue is post-fixed with osmium tannic acid paraphenylenediamine, prepared for epoxy resin sections, and stained with toluidine blue. **B.** Panoramic view of histology showing the RPE elevation from panel A (*yellow arrowheads*). **C.** Temporal to the RPE elevation, BALAD is narrow. **D.** Nasal to the RPE elevation, BALAD is wide. NFL, nerve fiber layer; GCL, ganglion cell layer; INL, inner nuclear layer; HFL, Henle fiber layer; ONL, outer nuclear layer; ONL/HFL, ONL and HFL indistinguishable due to *in vivo* dyslamination; IS, inner segments; OS, outer segments; BrM, Bruch's membrane; Ch, choroid.

Figure 7. Bacillary layer detachment associated with toxoplasmosis retinochoroiditis and Henle fiber layer schisis and edema.

A. Near-infrared reflectance (NIR, left) and spectral domain optical coherence tomography (SD-OCT, right) of a 14-year-old girl with a 10-day history of decreased visual acuity in her left eye. NIR shows a thin hyperreflective line (*black arrowheads*) indicating the margin of a bacillary layer detachment (BALAD). The

larger surrounding hyporeflective area corresponds to Henle fiber layer (HFL) schisis and edema on SD-OCT. SD-OCT (right) through the inferior macula demonstrates schisis and edema in the HFL (*white dashed arrow*). The green line indicates the location of the SD-OCT B-scan.

B. Adjacent superior SD-OCT B-scan shows a hyperreflective round structure within the HFL/outer nuclear layer that corresponds to the inferior margin of the BALAD. Schisis and edema of the HFL (*white dashed arrow*) are apparent on either side of the nascent BALAD.

C and D. Adjacent superior SD-OCT B-scan show a cystic cavity within the outer retinal layers that represents the posterior border of the BALAD. HFL schisis and edema (*white dashed arrows*) are apparent on either side of the BALAD.

E and F. Adjacent superior SD-OCT B-scan show a piriform-shaped BALAD. The ceiling of the BALAD (c-BALAD, *white arrowhead*) shows hyperreflective granularity. The floor of the BALAD (f-BALAD, *white arrowhead*) is continuous with the ellipsoid zone (EZ, *red arrowhead* in **F**) in adjacent attached retina and adherent to the retinal pigment epithelium-basal lamina-Bruch membrane complex (RBB, *yellow arrowhead* in **F**). HFL schisis and edema (*white dashed arrows*) are apparent on either side of the BALAD. No connecting fibers or strands are visible within the BALAD as opposed to the concurrent Henle fiber layer schisis and edema.

Table 1. Summary of Demographic Characteristics of Patients with Bacillary Layer Detachment from the Literature.

<i>Characteristics</i>	<i>Number (%)</i>
No. of patients	164
No. of eyes	178
Age (mean years \pm SD)	35.4 \pm 14.5
Gender n (%)	
Male	69/138 (50%)
Female	69/138 (50%)
Type of OCT n (%)	
SD-OCT	146/178 (82%)
TD-OCT	25/178 (14%)
SS-OCT	7/178 (4%)
Follow-up on OCT (mean days \pm SD)	167.4 \pm 134.3
Etiologies (n=22)	
VKH disease	77/164 (47%)
APMPPE	18/164 (11%)
Sympathetic ophthalmia	12/164 (7.3%)
Choroidal neovascularization	10/164 (6.2%)
Toxoplasmosis chorioretinitis	9/164 (5.5%)
Acute idiopathic maculopathy	9/164 (5.5%)
Immunotherapy-related toxicity	6/164 (3.7%)
Hematological disorders	4/164 (2.4%)
Posterior scleritis	3/164 (1.8%)
Choroidal metastasis	2/164 (1.2%)
Central serous chorioretinopathy	2/164 (1.2%)
Panretinal photocoagulation	2/164 (1.2%)
Peripapillary pachychoroid syndrome	1/164 (0.6%)
Ocular blunt trauma	1/164 (0.6%)
Uveal effusion syndrome	1/164 (0.6%)
Choroidal lymphoma	1/164 (0.6%)
Choroidal osteoma	1/164 (0.6%)
Chikungunya-associated uveitis	1/164 (0.6%)
Laser-induced maculopathy	1/164 (0.6%)
BDUMP	1/164 (0.6%)
Choroidal granuloma	1/164 (0.6%)
Preeclampsia	1/164 (0.6%)

Abbreviations: APMPPE: acute posterior multifocal placoid pigment epitheliopathy;

BDUMP: bilateral diffuse uveal melanocytic proliferation; OCT: optical coherence

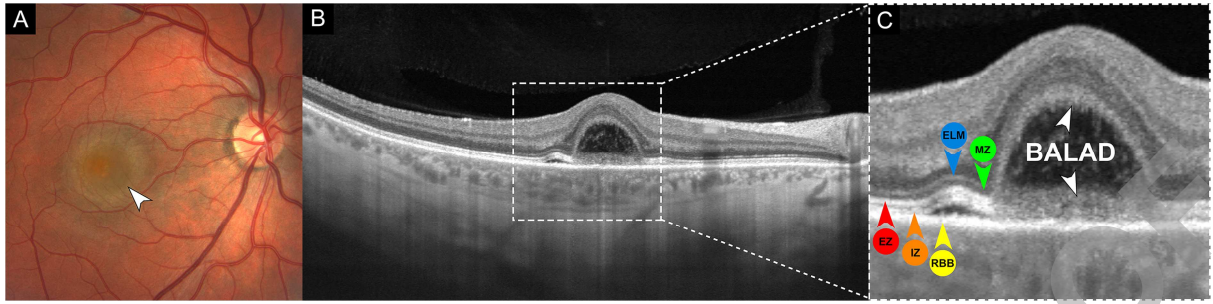
tomography; SD: spectral domain; SS: swept source; TD: time domain; VKH: Vogt-Koyanagi-Harada.

UNCORRECTED PROOF

Table 2. Optical Coherence Tomography and Related Multimodal Imaging Features of Bacillary Layer Detachment.

<i>Optical Coherence Tomography</i> <i>N=178 eyes</i>	<i>Ophthalmoscopy and Color Fundus Photography</i> <i>N=106 eyes</i>	<i>Fundus Autofluorescence</i> <i>N=22 eyes</i>	<i>Near-infrared Reflectance</i> <i>N=22 eyes</i>	<i>Fluorescein Angiography</i> <i>N=92 eyes</i>
<p>Intraretinal split at the level of the photoreceptor myoid zone</p> <p>Hyperreflective granular band forming the anterior border (ceiling) of the BALAD</p> <p>Faint, thickened, hyperreflective band delineating the posterior border (floor) of the BALAD and continuous with the EZ of adjacent attached retina</p> <p>Adherence of the BALAD floor with the RPE/Bruch's membrane complex and/or subretinal hyperreflective material</p> <p>Continuity of a second hyperreflective band below the BALAD floor with the interdigitation zone of adjacent attached retina (nearly half of cases)</p> <p>There may be edema/schisis present in the adjacent Henle fiber layer.</p> <p>Integrity of the external limiting membrane anterior to the BALAD (more than 70% of cases)</p> <p>High rate of suspended hyperreflective particles and medium internal optical intensity of the BALAD (more than 70% and 90% of cases, respectively)</p> <p>Distinctive piriform shape with acute angles at the base (more than 70% of cases)</p>	<p>Round or polygonal areas of presumed subretinal fluid (97.2%) displaying a characteristic yellow border (80.2%)</p> <p>Not visible on ophthalmoscopic examination (1%)</p> <p>Rarely multifocal (4.7%)</p>	<p>Hypoautofluorescence, presumably due to masking of RPE FAF by the intra-BALAD exudation, RPE disruption, or both (100%)</p>	<p>Hyporeflective lesions (100%) surrounded by a thin hyperreflective border (81.8%)</p>	<p>Varying degrees of hyperfluorescent dye pooling within the BALAD cavity (92.4%) with dark border visible in the late phase (72.4%). May resemble the angiographic appearance of a serous RPE detachment</p> <p>Not visible (7.6%)</p> <p>Associated findings: Optic disc and vascular staining, hyperfluorescent dye pooling beneath adjacent serous retinal detachments which typically show less distinct margins</p>

Abbreviations: BALAD: bacillary layer detachment; EZ; ellipsoid zone; FAF: Fundus autofluorescence; RPE: retinal pigment epithelium.



UNCORRECTED PROOF

